CrossMark

ORIGINAL PAPER

Renal stones composition in vivo determination: comparison between 100/Sn140 kV dual-energy CT and 120 kV single-energy CT

Matteo Bonatti[1] · Fabio Lombardo[2] · Giulia A. Zamboni[2] · Patrizia Pernter[1] · Armin Pycha[3] · Roberto Pozzi Mucelli[2] · Giampietro Bonatti[1]

Abstract The objective of this study is to compare in vivo, the accuracy of single-energy CT (SECT) and dual-energy CT (DECT) in renal stone characterization. Retrospective study approved by the IRB. 30 patients with symptomatic urolithiasis who underwent CT on a second-generation dual-source scanner with a protocol that included low-dose 120 kV scan followed by 100/Sn140 kV dual-energy scan have been included. Stone composition was classified as uric acid, cystine or calcium oxalates, and phosphates according to attenuation values at 120 kV and to 100/Sn140 kV attenuation ratios and compared with the infrared spectroscopy analysis. 50 stones were detected in 30 patients. SECT correctly assessed stone composition in 52 % of the cases, DECT in 90 %. Sensitivity, specificity, positive predictive value, and negative predictive value in differentiating uric acid vs. non-uric acid stones were 0.94, 0.72, 0.64, and 0.96 for SECT and 1.00, 0.94, 1.00, and 0.96 for DECT, respectively. DECT significantly performs better than SECT in characterising renal stones in vivo, and may represent a useful tool for treatment planning.

Keywords Multidetector-row computed tomography · Dual-energy CT · Urinary stones · Urolithiasis · Material decomposition · Urate

Introduction

Urolithiasis is a common disease, affecting about 12 % of men and 6 % of women during their lives, with a prevalence that is progressively increasing during the years and with high recurrence rate [1–5]. Urinary stones chemical composition is quite variable and comprehends, in the majority of the cases, calcium oxalates (monohydrate or dihydrate) or phosphates (brushite or apatite), uric acid, and cysteine [6]; moreover, mixed calculi may be often observed. Unenhanced CT is, nowadays, the imaging modality of choice in the evaluation of symptomatic urolithiasis, because of its ability of providing, by means of a single, rapid and reproducible examination, information about stone location and size, presence and degree of urinary obstruction, presence of complications, and eventual differential diagnoses [7–12].

Stone composition is a parameter that should be known to tailor the best therapeutic approach for each patient affected by symptomatic urolithiasis, since uric acid stones can be successfully managed by means of urine alkalinization that facilitates dissolution, struvite calculi are sensitive to extracorporeal shock-wave lithotripsy (ESWL), and calcium oxalate and cysteine stones often require percutaneous nephrolithotripsy or ureteroscopy [13]. Blood tests, urine sediment analysis, and review of patient's clinical history are often insufficient for determining the true nature of a calculus. In this setting, CT may represent a useful tool for stone composition characterization, being attenuation values correlated with stone composition [14–17]. However, no definite cut-off values have been provided in the literature for differentiating the various stone phenotypes, and a quite large variability in attenuation values has been reported by comparing different CT scanners [18, 19].

✉ Matteo Bonatti
matteobonatti@hotmail.com

1 Department of Radiology, Bolzano Central Hospital, 5 Boehler Street, 39100 Bolzano, Italy

2 Department of Radiology, University of Verona, 10 L.A. Scuro Place, 37134 Verona, Italy

3 Department of Urology, Bolzano Central Hospital, 5 Boehler Street, 39100 Bolzano, Italy

Table 1 CT scanning protocol in the suspicion of urolithiasis

Technique	kV	mAs Ref	Collimation (mm)	Rotation time (s)	Pitch	Dose reduction technique	Reconstruction thickness (mm)	Reconstruction algorithm	DLP (mGy/cm, median)	E (mSv, median)
Single energy	120	50	128 × 0.6	0.5	1.4	None	1.0	Iterative (SAFIRE® 3)	146	2.2
Dual energy	100/Sn140	162	32 × 0.6	0.5	0.7	Care DOSE 4D	1.0	FBP (D30f)	67	1.0

Since its introduction in the clinical practice, dual-energy CT (DECT) has emerged as an extremely accurate technique for determining urinary stones composition and several works have already demonstrated its high accuracy, both in vitro and in vivo [20–29]. Nevertheless, to our knowledge, there are no studies that have directly compared in vivo accuracy of DECT with that of single-energy CT in urinary stones characterisation.

Therefore, the aim of our study was to compare the accuracy in vivo of 100/Sn140 kV dual-energy CT with that of 120 kV single-energy CT in the determination of urinary stones composition by means of an automated commercially available software.

Materials and methods

Patient population

This was a retrospective study approved by our Institutional Review Board; need for informed consent was waived. We considered for the inclusion into our study 215 consecutive patients that underwent CT scan on the second-generation dual-source CT scanner in our institution in the clinical suspicion of urolithiasis during the period October 2012–April 2014.

Inclusion criteria were: presence of renal stones at CT (97/215 patients) and stones extraction or expulsion within 1 month from the CT examination with subsequent stone analysis by means of infrared spectroscopy (32/97).

Exclusion criteria were: incomplete CT examination (1/32 patients) and poor image quality, because of motion artefacts (1/32 patients). Therefore, our study population included 30 patients, 18 males and 12 females, with a mean age of 56 years (range 34–86).

CT protocol

All the examinations were performed on a second-generation dual-Source CT scanner (Somatom Definition Flash; Siemens Healthcare, Forchheim, Germany) equipped with a tin filter on the high-energy tube (Sn) for improved separation between the high- and low-energy spectra, according to a protocol that included a preliminary 120 kV single-energy low-dose scan of the abdomen, from the upper renal poles to the pelvic floor, followed by an additional 100/Sn140 kV simultaneous dual-energy scan limited to the volume(s) where urinary stones were eventually detected (Table 1). All the examinations were performed with the patient lying supine on the table, with the arms bended over his head whenever possible.
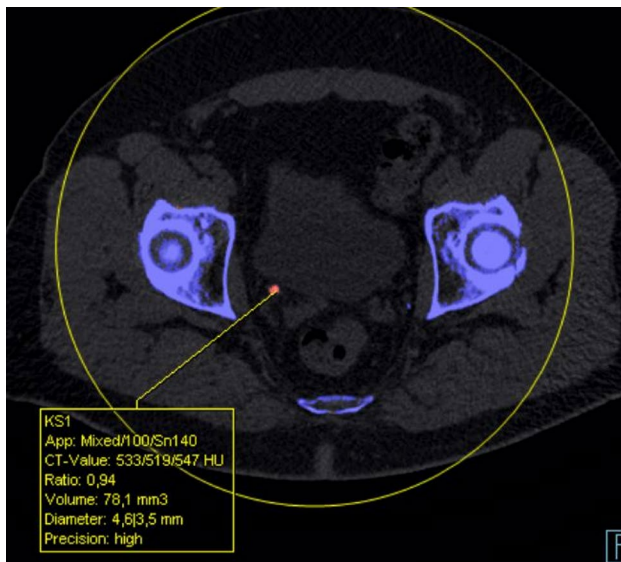
Image analysis

CT images were evaluated on a workstation (Syngo.Via, Siemens, Erlangen, Germany) by two radiologists with 5 and 15 years of experience in urogenital radiology, respectively, both with 4 years of experience in DECT, using multi-planar reconstructions.

First of all, the number of urinary stones, their location (urinary calices, pelvis, ureter, or bladder) and the presence of ureteral catheters was recorded by the two radiologists in consensus on the 120 kV images. Then, stone attenuation values (mean and standard deviation, in HU) at 120 kV were measured by the two radiologists independently on 1 mm-thick multi-planar reconstructions using a bone window ($L = 570$, $W = 2500$). Attenuation values were measured on magnified images by means of a round ROI that was drawn as large as possible to comprehend the largest stone area but no adjacent structures (Fig. 1). The data recorded by the two radiologists were used to calculate mean values and standard deviations, which were used for further analyses.

Further evaluations were performed on the 100/Sn140 kV data sets by means of a commercially available automated software (Syngo.Via CT Dual Energy—Kidney Stones, Siemens, Erlangen, Germany). Stone maximum diameter (mm), volume (mm³), attenuation values (mean and standard deviation, in HU) at 100, and Sn140 kV and 100/Sn140 kV attenuation ratios were calculated by the software (Fig. 2) and recorded. Moreover, stone colour on the automatically created colour-coded image (orange = uric acid stones; blue = non-uric acid stones) was annotated.
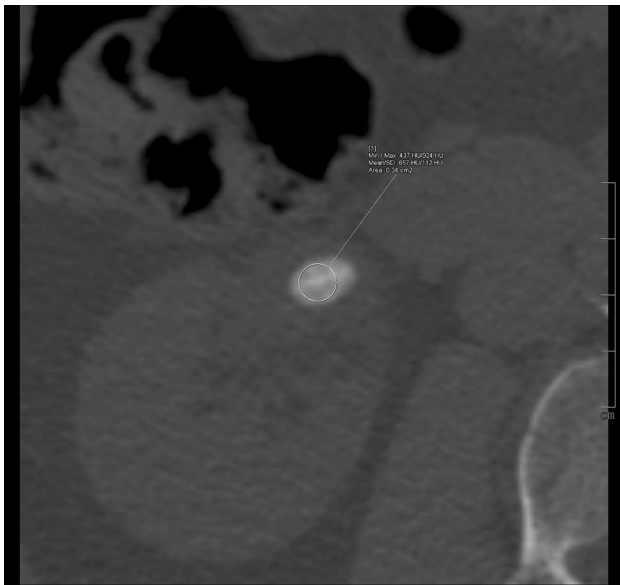
Fig. 1 Manual ROI placement for stone's attenuation assessment: a bone window must be used and the ROI must be drawn as large as possible, but it must not comprehend structures others than the stone itself

Fig. 2 Example of stone analysis performed by the automated software used in our study: information about stone's size, volume, attenuation at 100 and 120, and Sn140 kV and 100/Sn140 kV attenuation ratios were automatically provided. Moreover, the stone was colourcoded: *orange* for uric acid stones and *blue* for non-uric acid stones

On 120 kV single-energy images, according to the work by Mostafvi et al. [16], stones were considered mainly composed by uric acid if mean attenuation value was <538 HU, by cysteine if mean attenuation value was 538–1064 HU, and by calcium oxalates or phosphates if mean attenuation value was >1064 HU (Table 2). On 100/Sn140 kV dual-energy images, according to the producer's recommendations, stones were considered mainly composed by uric acid if 100/Sn140 kV attenuation ratio was <1.13, by cysteine if attenuation ratio was 1.13–1.24, and by calcium oxalates or phosphates if attenuation ratio was >1.24 (Table 3).

Finally, the two radiologists in consensus analysed dose reports for each patient.

For each examination, the following data were recorded: scan length (mm), CTDIvol (mGy), and DLP (mGy-cm). Effective dose (mSv) was also calculated using the formula $E = \mathrm{DLP} \times 0.015$.

Stone analysis

A research in our institutional database showed that 13/30 patients spontaneously expelled the stones and 17/30 underwent stone extraction by means of percutaneous nephrolithotripsy or ureteroscopy. The obtained stones were analysed by means of infrared spectroscopy and classified, according to their prevalent composition, into three categories: uric acid, cysteine, and calcific (calcium oxalates and phosphates). In case of patients presenting more than one stone, stone composition was considered the same for all the stones.

Statistical analysis

Sensitivity, specificity, positive predictive value (PPV), and negative predictive value (NPV) for both SECT and DECT in predicting renal stones composition were calculated with Fisher's test using a commercially available software (GraphPad Prism version 5.01 for Windows, GraphPad Software, San Diego California, USA, http://www.graphpad.com); accuracy was also calculated.

Results

50 stones were detected in 30 patients (range 1–4 stones per patient): 26 stones were located in the urinary calices, 15 in the ureters, 8 in the renal pelvis, and 1 in the urinary bladder.

At laboratory, 29/50 (58 %) stones were classified as prevalently composed by calcium oxalates or phosphates, 17/50 (34 %) by uric acid, and 4/50 (8 %) by cysteine.

Stones' attenuation values, as measured by the two radiologists on the 120 kV data set, are reported in Table 3. Moreover, Fig. 3 shows mean stone attenuation values, subdivided according to their prevalent composition, as found at infrared spectroscopy. 120 kV single-energy CT correctly assessed stone composition in 26/50 (52 %) of the

Table 2 CT cut-off values for renal stones characterization

	Single-energy CT, attenuation at 120 kV (HU)	Dual-energy CT, 100/Sn140 kV attenuation ratio
Uric acid	<538	<1.13
Cysteine	538–1064	1.13–1.24
Calcium oxalates/phosphates	>1064	>1.24

Table 3 Stones characterization by means of 120 kV single-energy CT

	Mean attenuation values at 120 kV (HU)	
	Reader 1	Reader 2
Uric acid stones	392 ± 44 (201–617)	392 ± 48 (177–577)
Cysteine stones	368 ± 83 (230–559)	424 ± 86 (291–552)
Calcium oxalates/phosophates stones	621 ± 97 (194–1266)	605 ± 87 (237–1343)
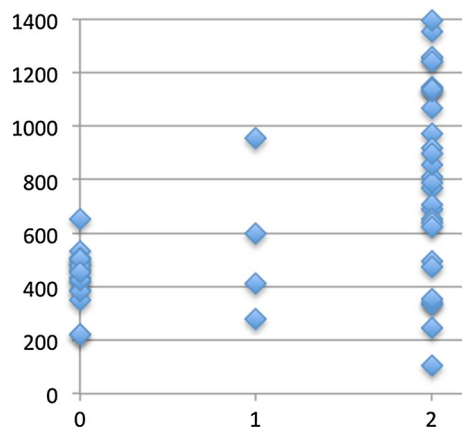
Fig. 3 Stones attenuation values (HU) at 120 kV single-energy CT, according to their prevalent composition at infrared spectroscopy

cases: 16/17 uric acid stones were correctly characterized by SECT, while 1/17 was mistakenly characterized as composed by cysteine, 2 out of the 4 cysteine stones were correctly characterized by SECT, whereas 2/4 were mistakenly characterized as composed by uric acid, and 8/29 calcium oxalates or phosphates stones were correctly characterized by SECT, whereas 14/29 were mistakenly characterized as composed by cysteine and 7/29 by uric acid. No statistically significant differences were observed in stone maximum diameter between the stones characterized correctly and incorrectly.

Stones mean maximum diameter, volume, and attenuation values, as calculated by the automated software on the 100/Sn140 kV data sets, are reported in Table 4; no statistically significant differences in stone maximum diameter were observed between the three groups.

Moreover, Fig. 4 shows stones 100/Sn140 kV attenuation ratios, subdivided according to their prevalent composition, as found at infrared spectroscopy. Dual-energy CT correctly assessed stone composition in 45/50 (90 %) of the cases: all 17 uric-acid-composed stones were correctly characterized by DECT, 2 out of the 4 cysteine stones were correctly characterized by DECT, whereas 2/4 were mistakenly characterized as composed by calcium oxalates or phosphates, and 26 out of the 29 calcium oxalates were correctly characterized by DECT, whereas 1/29 was characterized as composed by cysteine and 2/29 were characterized as composed by uric acid. Results of stones' characterization were concordant between SECT and DECT in 24/50 (48 %) of the cases.

Single-energy CT correctly differentiated uric acid vs. non-uric acid stones in 40/50 (80 %) of the cases, whereas dual-energy CT in 48/50 (96 %) of the cases. No statistically significant differences were observed in maximum diameters between uric acid stones and non-uric acid stones. Sensitivity, specificity, positive predictive value, and negative predicting value for both SECT and DECT in predicting uric-acid renal stones composition are reported in Table 5.

Table 4 Stones characterization by means of 100/Sn140 kV dual-energy CT

	Mean diameter (mm)	Mean volume (mm3)	Mean attenuation values at 100 kV (HU)	Mean attenuation values at Sn140 kV (HU)	Mean ratio 100/Sn140 kV
Uric acid stones	7 (3.3–14)	138 (6–320)	430 ± 56 (217–669)	440 ± 70 (221–508)	0.97 (0.89–1.05)
Cysteine stones	7 (1–24)	353 (2–1390)	323 ± 52 (301–1063)	499 ± 57 (258–843)	1.24 (1.17–1.28)
Calcium oxalates/phosophates stones	5 (2–13)	97 (3–490)	936 ± 90 (121–1645)	703 ± 84 (91–1391)	1.35 (0.94–1.69)
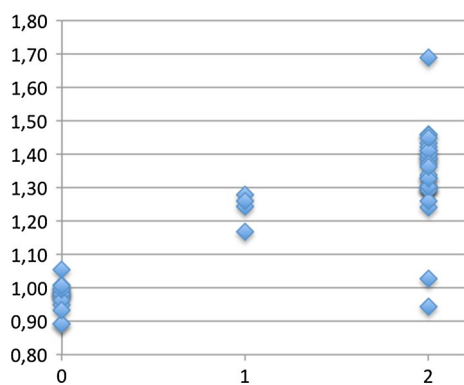
Fig. 4 Stones attenuation ratios at 100/Sn140 kV dual-energy CT, according to their prevalent composition at infrared spectroscopy

Table 5 Performance of single-energy CT and of dual-energy CT in the recognition of uric acid stones

	Single-energy CT (%)	Dual-energy CT (%)
Sensitivity	94.12	100
Specificity	72.73	93.94
Positive predictive value (PPV)	64	89.47
Negative predictive value (NPV)	96	100
Accuracy	80	96

Mean DLP and effective dose (ED) for the preliminary 120 kV scan were 146 mGy-cm (128–174) and 2.2 mSv (1.9–2.6), respectively. Mean DLP and ED for the added DE scans were 67 mGy-cm (52–72) and 1.0 mSv (0.8–1.1), respectively.

Discussion

The first dual-energy CT experiences are dated back to the late 1970s. In the last decades, various CT scanners have been developed to obtain dual-energy data sets with different techniques. Dual-source dual-energy scanners, single-source dual-energy scanners, single-source dual-energy scanners with fast kV switching, and single-source dual-energy scanners with dual detector layer are currently available from different vendors.

Computed tomography represents, nowadays, the imaging modality of choice in the evaluation of patients with suspected urolithiasis. Besides information about the presence of stones, their location, and the eventual presence of complications, CT has also shown to be useful for urinary stones composition characterization; indeed, a strict correlation between stones' attenuation values and their chemical composition has been highlighted by other authors [14].

In our series, however, CT attenuation values have demonstrated to be unsatisfactory correlated with stones' composition (accuracy 52 %) and we have found a lot of overlap between different stone types; in particular, about an half of the calcified stones have shown attenuation values that were comparable with those of uric acid and cysteine ones. A further subanalysis has demonstrated that SECT errors in stones characterization were not correlated with their size; however, in our series, only three stones had a minimum diameter <2 mm, below which partial volume artefacts are most likely to influence HU values determination. On the other hand, our work has demonstrated that dual-energy CT has a high accuracy (90 %) in differentiating the different stone types, performing significantly better than single-energy CT for this aim.

The performances of both SECT and DECT increased if stones' composition analysis was limited to the differentiation between uric acid and non-uric acid stones, which is also the most relevant information that urologist want to know to tailor the best therapeutic approach; indeed, uric acid stones may be easily dissolved by medical treatment with urine alkalinisation.

SECT correctly differentiated uric acid from non-uric acid stones with a satisfactory accuracy (0.80), but its specificity in recognising uric acid stones was fair (0.73), with a positive predictive value of only 0.64; this may represent a limit to its clinical use, because it may lead to medically treat a group of patients who will not have any benefit from this approach. On the other hand, DECT accuracy in differentiating uric acid and non-uric acid stones was extremely high (0.96), with specificity and PPV of 0.94 and 0.89, respectively; in our series, only two stones were incorrectly classified by DECT: in both cases, the automated software characterized the stones as prevalently composed by uric acid, whereas they were composed by calcium oxalates/phosphates at infrared spectroscopy. Both mistakenly classified stones were located in the ureters, and a JJ ureteral catheter was already in place at the time of CT scan (Fig. 5). This suggests that the presence of a ureteral catheter next to a stone may introduce a certain degree of error in its DECT characterization by means of an automated software, probably due to beam-hardening artefacts caused by JJ catheter itself; on the other hand, differentiation between uric acid and non-uric acid stone partially loses its importance if the stone has already reached the ureter, and a JJ catheter is already in place. In both cases, manual measurement of stone's attenuation values by means of a round ROI on separated 100 kV and Sn140 kV images and attenuation ratio manual calculation correctly classified the stones as "non-uric acid".

Another aspect to take into consideration is the added dose given to the patient for dual-energy acquisitions, which, in our series, was in the order of 1 mSv. Although
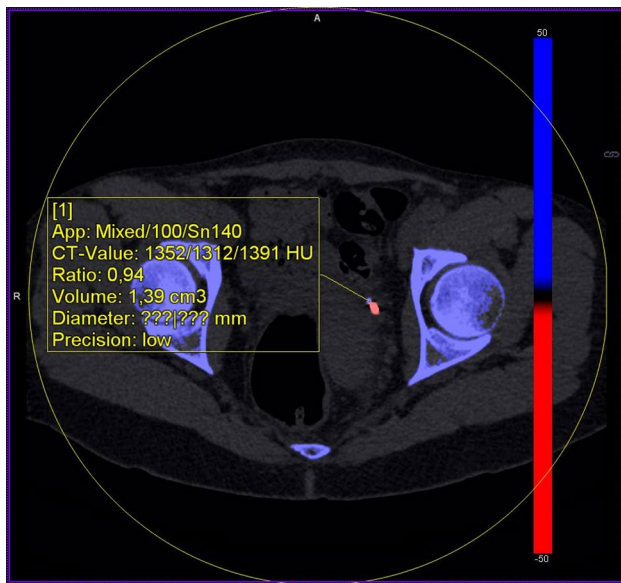
Fig. 5 Stone incorrectly characterized by the automated software. This small stone located next to a ureteral catheter (*orange*) was characterized as uric acid by the automated software, according to its low 100/Sn140 kV attenuation ratio, whereas infrared spectroscopy characterized it as composed by calcium oxalates. In any case, the automated software colour-coded it in blue (non-uric acid), because of its high attenuation

it cannot be considered an unremarkable dose, a correct preoperative characterization of the calculus is fundamental to distinguish the patients who might take advantage from medical therapy from those who would require an interventional approach, possibly avoiding unnecessary invasive procedures and possible complications.

Our study had some limitations. First of all, at 120 kV, we classified the stones according to the density values proposed by Mostafvi et al., which were found out using a GE-scanner, as, to our knowledge, there are no papers that report similar data for Siemens' ones; this might represent a limitation according the work by Grosjean et al. [18] that highlighted a significant variability in urinary stones CT attenuation values using different scanners. Second, our study population was relatively small, because stone analysis by means of infrared spectroscopy was not available for the majority of patients, in which CT showed the presence of urinary calculi. This was due to the high number of patients that spontaneously expelled the calculus and did not provide it to the laboratory for further analysis. Image quality of the dual-energy acquisition was also judged inadequate in one patient, due to motion artefacts. Finally, we did not consider the presence of mixed stones, classifying the stones only on the base of their prevalent composition; further studies are needed to evaluate the accuracy of DECT in discerning the different components of mixed stones.

In conclusion, dual-energy CT performs significantly better than single-energy CT in renal stone composition determination and reliably discriminates between uric acid and non-uric acid stones. Furthermore, the potential benefits of preoperative characterization of renal stones largely exceed the low risk related to the added radiation dose given to the patient for dual-energy acquisitions.

References

1. Lotan Y (2009) Economics and cost of care of stone disease. Adv Chronic Kidney Dis 16:5–10
2. Curhan GC (2007) Epidemiology of stone disease. Urol Clin N Am 34:287–293
3. Trinchieri A, Coppi F, Montanari E, Del Nero A, Zanetti G, Pisani E (2000) Increase in the prevalence of symptomatic upper urinary tract stones during the last ten years. Eur Urol 37:23–25
4. Trinchieri A (1996) Epidemiology of urolithiasis. Archivio italiano di urologia, andrologia: organo ufficiale [di] Societa italiana di ecografia urologica e nefrologica/Associazione ricerche in urologia 68:203–249
5. Trinchieri A (2008) Epidemiology of urolithiasis: an update. Clin Cases Miner Bone Metab Off J Ital Soc Osteoporos Miner Metab Skelet Dis 5:101–106
6. Saita A, Bonaccorsi A, Motta M (2007) Stone composition: where do we stand? Urol Int 79(Suppl 1):16–19
7. Boulay I, Holtz P, Foley WD, White B, Begun FP (1999) Ureteral calculi: diagnostic efficacy of helical CT and implications for treatment of patients. AJR Am J Roentgenol 172:1485–1490
8. Dalla Palma L, Pozzi-Mucelli R, Stacul F (2001) Present-day imaging of patients with renal colic. Eur Radiol 11:4–17
9. Heneghan JP, McGuire KA, Leder RA, DeLong DM, Yoshizumi T, Nelson RC (2003) Helical CT for nephrolithiasis and ureterolithiasis: comparison of conventional and reduced radiation-dose techniques. Radiology 229:575–580
10. Tamm EP, Silverman PM, Shuman WP (2003) Evaluation of the patient with flank pain and possible ureteral calculus. Radiology 228:319–329
11. Alessi V, Avenia S, Bianco BP, Cassano T, Pappalardo MP, Rossello M (2001) Helical CT without contrast media as alternative to other methods in urolithiasis. Radiol Med (Torino) 101:466–476
12. Tartari S, Rizzati R, Righi R, Deledda A, Terrani S, Benea G (2010) Low-dose unenhanced CT protocols according to individual body size for evaluating suspected renal colic: cumulative radiation exposures. Radiol Med (Torino) 115:105–114
13. Kambadakone AR, Eisner BH, Catalano OA, Sahani DV (2010) New and evolving concepts in the imaging and management of

urolithiasis: urologists' perspective. Radiogr Rev Publ Radiol Soc N Am Inc 30:603–623

14. Nakada SY, Hoff DG, Attai S, Heisey D, Blankenbaker D, Pozniak M (2000) Determination of stone composition by non-contrast spiral computed tomography in the clinical setting. Urology 55:816–819

15. Saw KC, McAteer JA, Monga AG, Chua GT, Lingeman JE, Williams JC Jr (2000) Helical CT of urinary calculi: effect of stone composition, stone size, and scan collimation. AJR Am J Roentgenol 175:329–332

16. Mostafavi MR, Ernst RD, Saltzman B (1998) Accurate determination of chemical composition of urinary calculi by spiral computerized tomography. J Urol 159:673–675

17. Hillman BJ, Drach GW, Tracey P, Gaines JA (1984) Computed tomographic analysis of renal calculi. AJR Am J Roentgenol 142:549–552

18. Grosjean R, Daudon M, Chammas MF Jr et al (2013) Pitfalls in urinary stone identification using CT attenuation values: are we getting the same information on different scanner models? Eur J Radiol 82:1201–1206

19. Motley G, Dalrymple N, Keesling C, Fischer J, Harmon W (2001) Hounsfield unit density in the determination of urinary stone composition. Urology 58:170–173

20. Boll DT, Patil NA, Paulson EK et al (2009) Renal stone assessment with dual-energy multidetector CT and advanced post-processing techniques: improved characterization of renal stone composition—pilot study. Radiology 250:813–820

21. Matlaga BR, Kawamoto S, Fishman E (2008) Dual source computed tomography: a novel technique to determine stone composition. Urology 72:1164–1168

22. Stolzmann P, Kozomara M, Chuck N et al (2010) In vivo identification of uric acid stones with dual-energy CT: diagnostic performance evaluation in patients. Abdom Imaging 35:629–635

23. Stolzmann P, Scheffel H, Rentsch K et al (2008) Dual-energy computed tomography for the differentiation of uric acid stones: ex vivo performance evaluation. Urol Res 36:133–138

24. Thomas C, Patschan O, Ketelsen D et al (2009) Dual-energy CT for the characterization of urinary calculi: in vitro and in vivo evaluation of a low-dose scanning protocol. Eur Radiol 19:1553–1559

25. Eliahou R, Hidas G, Duvdevani M, Sosna J (2010) Determination of renal stone composition with dual-energy computed tomography: an emerging application. Semin Ultrasound CT MR 31:315–320

26. Hidas G, Eliahou R, Duvdevani M et al (2010) Determination of renal stone composition with dual-energy CT: in vivo analysis and comparison with X-ray diffraction. Radiology 257:394–401

27. Manglaviti G, Tresoldi S, Guerrer CS et al (2011) In vivo evaluation of the chemical composition of urinary stones using dual-energy CT. AJR Am J Roentgenol 197:W76–W83

28. Thomas C, Heuschmid M, Schilling D et al (2010) Urinary calculi composed of uric acid, cystine, and mineral salts: differentiation with dual-energy CT at a radiation dose comparable to that of intravenous pyelography. Radiology 257:402–409

29. Thomas C, Krauss B, Ketelsen D et al (2010) Differentiation of urinary calculi with dual energy CT: effect of spectral shaping by high energy tin filtration. Invest Radiol 45:393–398